JOURNAL OF PROPULSION AND POWER
Vol. 18, No. 3, May–June 2002

Aerodynamic Optimization of Turbomachinery Cascades Using Euler/Boundary-Layer Coupled Genetic Algorithms

Ozhan Oksuz,* I. Sinan Akmandor,† and Mehmet S. Kavsaoglu‡
Middle East Technical University, 06531 Ankara, Turkey

A new methodology is developed to find the optimal aerodynamic performance of a turbine cascade. A boundary-layer coupled Euler algorithm and a genetic algorithm are linked within an automated optimization loop. The multiparameter objective function is based on the blade loading. For a given inlet Mach number and baseline cascade geometry, the flow inlet and exit angles, the blade thickness and the solidity are optimized by a robust genetic algorithm. First, the Sanz subcritical turbine cascade is selected as the baseline cascade and is used for flow solver validation. Second, the baseline cascade parameters are modified to yield the maximum tangential blade force. Finally, the effects of different crossover techniques, random number seeds, and population sizes on the performance of the genetic algorithm are studied. It is shown that the maximum blade loading is achieved for a higher flow turning, a wider pitch, and a thicker cascade.

Nomenclature

C_D	=	drag coefficient
C_{disp}	=	dissipation coefficient
C_f	=	friction coefficient
C_L	=	lift coefficient
c	=	blade chord
$\mathrm{d}s$	=	differential surface area
H	=	shape parameter
h_t	=	total enthalpy
L	=	lift
M_{e_a}	=	average Mach number at the edge of the boundary layer
n	=	population size
$\boldsymbol{n}$	=	unit vector normal to computational streamline cell face
p	=	pressure
$\boldsymbol{q}$	=	relative velocity vector
s	=	solidity
t	=	blade thickness
u_e	=	streamvise velocity at the edge of the boundary layer
Y	=	blade loading
β_{exit}	=	exit flow angle
β_{inlet}	=	inlet flow angle
β_m	=	mean flow angle
γ	=	ratio of specific heats
δ^*	=	displacement thickness
δ^{**}	=	density thickness
θ	=	momentum thickness
θ^*	=	kinetic energy thickness
ξ	=	streamwise coordinate
ρ	=	density

Introduction

THE numerical simulation of turbine cascades has been extensively improved over the last 20 years. Despite limitation as a result of modeling approximations such as turbulence and transition modeling, cooling and heat-transfer calculations, these methods are now capable of analyzing the performance of turbine blades with a flow accuracy that is acceptable for most engineering purposes. Computational fluid dynamics has also matured to the point at which it is widely used as a key tool for aerodynamic design. However for the final design process most designers still adopt a "trial and error" approach, analyzing the current design, and modifying it in function of the computational results or the experimental data, according to empirical rules or to their own experience. Numerical optimization methods aim to shorten and simplify this iterative process, while significantly improving the design output. All optimization problems contain three components:

1) Objectives describe what one hopes to achieve through the optimization process. In this paper the objective function is set to be the cascade tangential force.

2) Optimization parameters describe how the system is to be adjusted in order to best meet the objectives. Parameters that determine the shape of the boundary are an example. In this study the optimization parameters are blade thickness, blade pitch, flow inlet and exit angles. The cascade geometry is modified accordingly.

3) Constraints guide the optimization through states that must be satisfied. In our case these are the cascade geometry limitations. Moreover, an additional drag coefficient constrained is implemented for comparison.

Optimization techniques can be classified in three categories: local, global, or other methods. Local methods are gradient-based algorithms, which only search one part of the design space and stop after finding a local optimum. Adjoint, single, or multigrid preconditioners, alternating direction implicit methods are all local methods.[1] Global methods are stochastic methods that take into consideration the entire design space. Genetic algorithms, simulated annealing, random search methods are all considered as global methods. They also have the advantage of operating on discontinuous design spaces. Other optimization algorithms that do not fall entirely within either of these two categories are one-shot or inverse methods.[2]

The objective of the present paper is to develop an automated optimization loop by using the very fast and accurate two-dimensional Euler/boundary-layer coupled flow analysis methodology of Giles and Drela[3] and Drela[4] together with a genetic algorithm. The second-order-accurate Newton–Raphson algorithm consists of a two-dimensional finite volume steady Euler flow solver strongly coupled to a set of multilayer integral boundary-layer equations. The flow algorithm has already been successfully used in the analysis and design of turbomachinery blades and wind turbine cascades.[5,6] The present optimization aims to achieve a highly loaded blade section by modifying the baseline Sanz subcritical turbine cascade.[7]

Presented as Paper 2001-2597 at the AIAA CFD Conference, Anaheim, CA, 11–14 June 2001; received 6 August 2001; revision received 28 January 2002; accepted for publication 30 January 2002.

*Research Assistant, Department of Aerospace Engineering; ozhan@ae.metu.edu.tr.

†Professor, Department of Aerospace Engineering; akmandor@metu.edu.tr. Member AIAA.

‡Associate Professor, Department of Aerospace Engineering; kavsa@metu.edu.tr. Senior Member AIAA.

Euler/Boundary-Layer Coupled Flow Solver

The second-order-accurate cell-face centered implicit finite volume scheme uses the Newton linearized integral forms of the governing equations. The flow domain is discretized on an intrinsic streamline grid. The computational domain is in the absolute stationary frame of reference where total enthalpy is conserved. The initial streamlined grid is obtained from an elliptic grid generator and corresponds to an incompressible flow solution. As the numerical solution is iterated, the flow variables and the node positions are updated allowing the streamline grid to adapt to the flow physics. At transonic regions artificial compressibility is used so as to upwind the density in the continuity equation. Accordingly, the upstream region of dependence is properly taken into account, and the character of the steady governing equations is modified. The continuity, momentum and energy equations are expressed as

$$\oint \rho \boldsymbol{q} \cdot \boldsymbol{n}\, \mathrm{d}s = 0 \tag{1}$$

$$\oint [\rho (\boldsymbol{q} \cdot \boldsymbol{n})\boldsymbol{q} + p\boldsymbol{n}]\, \mathrm{d}s = 0 \tag{2}$$

$$\oint \rho \boldsymbol{q} \cdot \boldsymbol{n} h_t\, \mathrm{d}s = 0 \tag{3}$$

In the energy equation the total enthalpy is defined as

$$h_t = \gamma/(\gamma - 1)(p/\rho) + q^2/2 \tag{4}$$

These governing equations are solved simultaneously with the boundary-layer equations representing the momentum and the shape parameter equations, namely,

$$\frac{\ell n(\theta_2/\theta_1)}{\ell n(\xi_2/\xi_1)} - \frac{C_f}{2}\frac{\xi_a}{\theta_a} + \left(H_a + 2 - M_{e_a}^2\right)\frac{\ell n(u_{e2}/u_{e1})}{\ell n(\xi_2/\xi_1)} = 0 \tag{5}$$

$$\frac{\ell n\left(H_2^*/H_1^*\right)}{\ell n(\xi_2/\xi_1)} + \frac{\xi_a}{\theta_a}\left(\frac{C_f}{2} - \frac{2C_{\mathrm{disp}}}{H_a^*}\right) + \left(\frac{2H_a^{**}}{H_a^*} + 1 - H_a\right)\frac{\ell n(u_{e2}/u_{e1})}{\ell n(\xi_2/\xi_1)} = 0 \tag{6}$$

In Eqs. (5) and (6) given H, H^*, H^{**} are the shape parameters based on δ^*, θ^*, and δ^{**}, respectively. Subscripts 1, 2, a describe the inlet, the exit, and the average values of the control volume, respectively.

Inflow

The inlet boundary condition specifies the Mach number and the stagnation enthalpy for each streamtube. Together with a given inlet geometry, this defines the mass passing through each streamtube. Moreover, the inlet streamtube slope is also specified.

Outflow

For fully subsonic flows no thermodynamic variables are specified at the exit. The outlet streamline slope is also not specified because this variable is already constrained by the Kutta condition, which is explicitly imposed as a constraint variable.

Blade

The streamtube that defines the surface of the airfoil is considered to be an impermeable wall contour. Along this boundary the solid wall condition simply states that the nodes along the pressure and suction side do not move.

Genetic Algorithm

Genetic algorithms (GA) are search algorithms that mimic the behavior of natural selection to find the global optimum point in a given design space. GA procedure can climb many peaks in parallel; thus the probability of finding a local peak instead of the global is reduced significantly with GAs as compared with the conventional methods that search from a point to another point like the gradient-based methods. The optimization algorithm modifies the Sanz subcritical cascade by changing the optimization parameters that are blade inlet and exit flow angles, cascade thickness, and solidity. Then, the coupled flow solver calculates the objective function value, which is the tangential blade force and sends it to the GA. Accordingly, GA uses this value to assign a fitness to each geometry. The corresponding automated optimization flow chart is given in Fig. 1.

The tangential blade force on a blade section is expressed as

$$Y = L\cos\beta_m[1 + (C_D/C_L)\tan\beta_m] \tag{7}$$

The mean flow angle β_m is defined by

$$\tan\beta_m = \tfrac{1}{2}(\tan\beta_{\mathrm{inlet}} + \tan\beta_{\mathrm{exit}}) \tag{8}$$

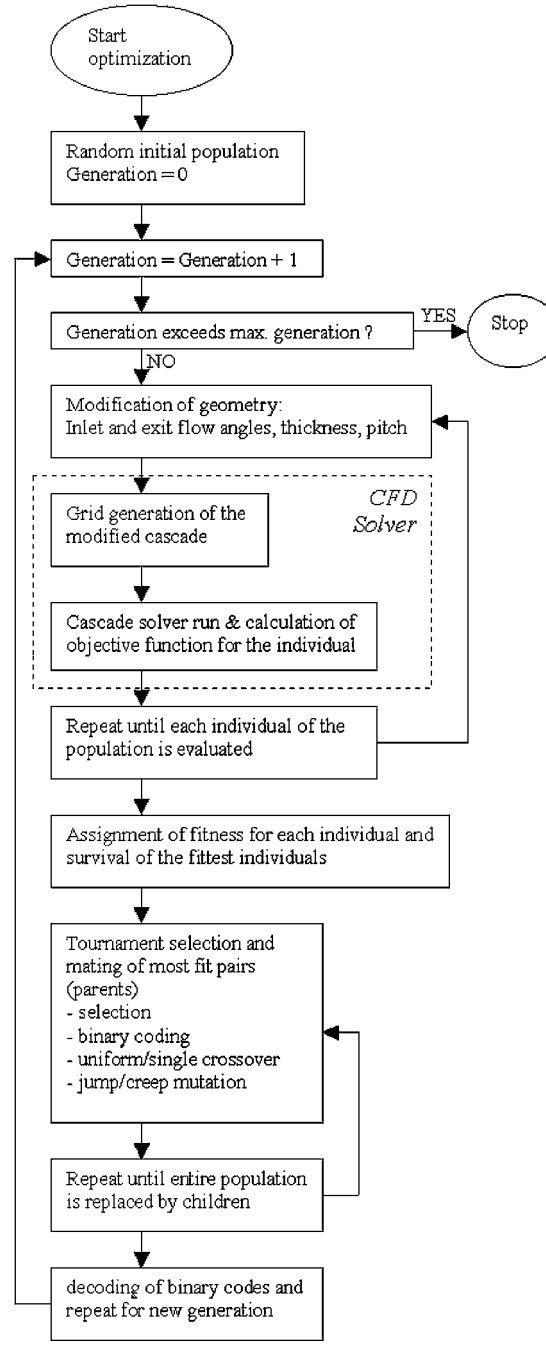

Fig. 1 Automated optimization flowchart.

For the parametrical change of inlet and exit flow angles, blade thickness and cascade solidity, this equation identifies the force to be maximized. Each one of the cascade geometries associated to a flow configuration is called an individual of a generation. The range of each of these parameters are arbitrarily constrained by the design space:

Inlet flow angle:

$$0 \text{ deg} < \beta_{\text{inlet}} < 10 \text{ deg}$$

Outlet flow angle:

$$0 \text{ deg} < \beta_{\text{exit}} < 70 \text{ deg}$$

Solidity:

$$0.3 < s < 2.5$$

Thickness-to-chord ratio:

$$0.05 < t/c < 0.5$$

The smooth bending of the baseline cascade camber to obtain a predetermined blade exit angle and the modification of the blade thickness are illustrated in Fig. 2. The inlet Mach number ($M_0 = 0.343$) and the cascade axial chord ($c = 1$) are held fixed while evaluating the tangential forces of reshaped blade sections. The calculated forces are subsequently analyzed by the optimization algorithm, which evolutionarily approaches the maximum turbine blade loading.

The GA works from a rich database of cascades forming a population. By using crossover and mutation operations, the forthcoming population evolves toward better solutions having higher tangential force. Each parameter set defines a cascade configuration with a corresponding binary string so called a chromosome. The real value of each design parameter is expressed as a string of binary digits, for example, 101101. The associated chromosome for a specific cascade is formed by placing the binary digits corresponding to each parameter back to back in one string. For example, if blade inlet and exit angles, blade thickness, and solidity values were binary coded as 001100, 010101, 001011, and 110001, respectively, then the chromosome string would be 001100010101001011110001.

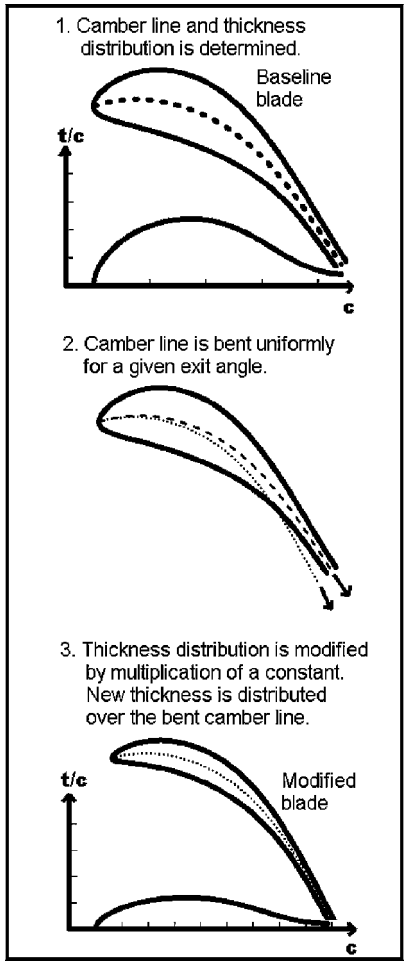

Fig. 2 Modification of the cascade geometry.

Our GA is composed of three operators[8]: reproduction, crossover, and mutation.

Reproduction is a process in which cascades are selected according to their fitness values. This implies that a cascade with a higher fitness value (tangential force) has a higher probability of contributing in the next generation. After assigning the fitness to each cascade configuration, selection for mating is performed by a tournament selection method.[9] Moreover, elitism (that is, best individual replicated into next generation) is invoked. This ensures the survival of the best individual from each generation.

Crossover proceeds in two steps. First, selected cascades are coupled at random. Second, each pair of cascades undergoes a partial exchange of their chromosomes at a random crossing site with a probability. This results in a pair of individuals of a new generation. For example,

$$\left.\begin{aligned} C_1 &: 10100011 \\ C_2 &: \underline{11110111} \end{aligned}\right\} \Rightarrow \begin{cases} C_1' : 1010\underline{0111} \\ C_2' : \underline{1111}0011 \end{cases}$$

Parents 1 and 2 are mated, and children $1'$ and $2'$ are obtained. The chromosomes C_1' and C_2' now correspond to two new blade configurations with different blade inlet and exit flow angles, cascade thickness, and solidity.

Mutation is a bit change of a chromosome that occurs during the crossover process. Mutation implies a random walk through the string space and plays a secondary role in the GA. For example, the child $1'$ might be faced with a mutation like

$$C_1' : 10100111 \Rightarrow C_1' : 11100111$$

on the second bit of its chromosome.

Successive generations are created by crossover, mutation, and reproduction operators, until very fit cascades are obtained in the population.

Diversity of the cascade population heavily depends on the crossover and mutation probabilities. In this study the crossover probability is set at 50%, which is the usual case for genetic algorithm studies.[8] On the other hand, the probability of mutation is particularly low, selected in consistence with the literature[8] as "1/(chromosome length)." The probability of mutation is selected as 2%.

Results and Discussion

Test Case and Baseline Cascade

Sanz subcritical turbine cascade is selected as the test and baseline cascade. The flow solver is validated using the Sanz subcritical cascade incompressible flow results that are obtained by hodograph related methods with boundary-layer corrections.[7] The first column of Table 1 summarizes the main flow and geometrical properties of the Sanz subcritical turbine cascade as well as the cascade performance results. The Reynolds number is taken as 6×10^6. The laminar-turbulent boundary-layer transition points on the pressure and suction sides are both arbitrarily set at 15% of the chord distance away from the leading edge. A flow adapting streamline grid of 82×19 nodes is used.

The analytical and numerical blade section surface Mach-number distributions are given in Fig. 3. The agreement is apparent. The exit flow angle is also numerically determined through the Kutta condition applied at the trailing edge. Accordingly, the calculated flow turning is 95.15 deg as compared to the Sanz's exact value of 93.35 deg. Although the Sanz supercritical turbine cascade[10] geometry and related input are not used in the optimization process, it has been included in Table 1 for comparison purpose.

Table 1 Performance comparison of turbine cascades

Characteristics	Baseline cascade: Sanz subcritical[7]	Sanz supercritical cascade[10]	Optimized cascade	Optimized cascade C_D constrained
Inlet Mach number	0,343	0,343	0,343	0,343
Inlet flow angle, deg	36,00	38,13	34,21	34,50
Exit flow angle, deg	−57,35	−56,93	−56,85	−55,87
Solidity	1,497	0,742	0,936	0,587
Thickness/Chord	0,228	0,202	0,427	0,264
Results				
C_L	1,966	3,969	4,312	2,606
C_D	1,858	2,335	4,310	1,888
Zweifel's criterion	0,7536	1,476	1,561	1,667
Blade loading	0,1324	0,2098	0,2970	0,1499

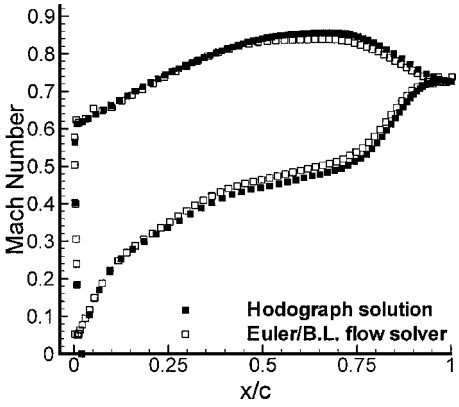

Fig. 3 Surface Mach-number distribution for Sanz subcritical cascade.

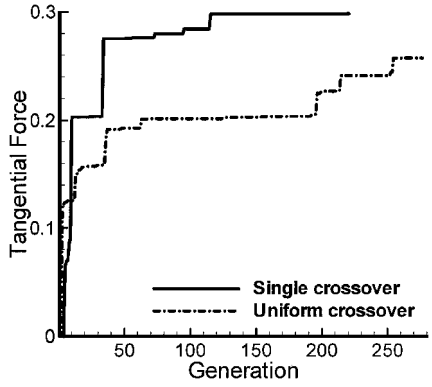

Fig. 4 Effect of crossover on the GA performance.

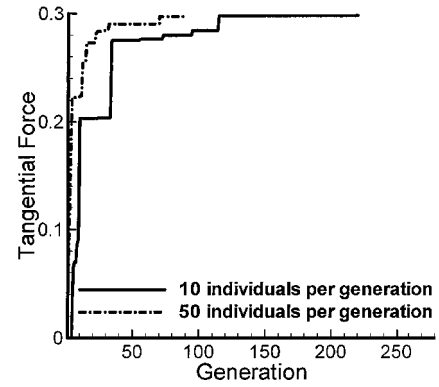

Fig. 5 Effect of population size on the GA performance.

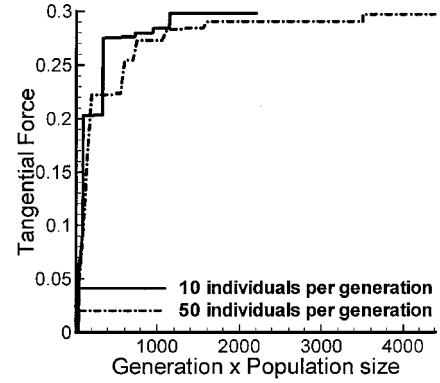

Fig. 6 Computational cost incurred by the population size.

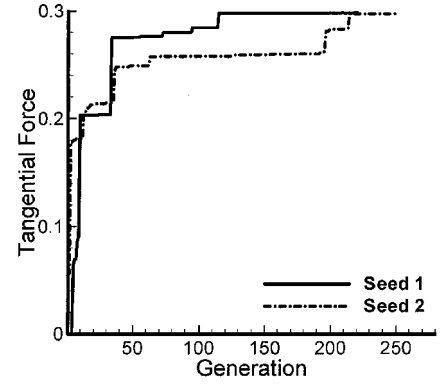

Fig. 7 Effect of random seed on the GA performance.

Performance of the Genetic Optimization as Applied to the Turbine Cascade

Crossover type, population size, and behavior according to different seeds are the main factors playing a key role on the performance of a genetic algorithm. The effects of uniform vs single crossover, 10-member vs 50-member generations, and two logically different random seed numbers are studied in this paper.

Uniform crossover operates on each chromosome bit position, swapping the bit values between the pair of mating strings with a given probability. Whereas single crossover is the simplest one, only one crossover point is selected randomly, and the codes are swapped. While expecting the single-point crossover method to limit the diversity of the population, Fig. 4 shows that single crossover generations allow a faster convergence to optimum cascade configuration, when compared to uniform crossover.

Next, the effect of population size is analyzed. The convergence of the objective function is shown in Figs. 5 and 6. The first run of GA is made with a population size of 10 individuals. The optimized blade loading is not quite reached even after the first 150 generations (Fig. 5). On the other hand, when the optimization is undertaken with a population size of 50 individuals, the optimum loading is reached in less than 50 generations. However, this huge difference in the generation number can be misleading if the computational time between the two optimizations is not compared. Numerical experimentation showed that the CPU time spent for the population generation is negligible when compared to the flow solution CPU time of one individual. Therefore, the run time of a 50-member population can be considered to be equivalent to the run time of five evaluations for a 10-member population. So, a supplementary figure based on the product of generation and population size is shown in Fig. 6 to represent the computational cost incurred for both population sizes. Interestingly, in the design space small populations perform better than large populations.

The effect of initial seed on the optimization process is illustrated by Fig. 7. Two randomly seeded optimization runs tend to converge toward each other as the number of generations increases, even though they follow different paths. Indeed, after sufficient

generations this effect tends to disappear, indicating the robustness of the optimization technique.

The dependence of the genetic algorithms to these parameters is studied quite a lot. Whether the best solution has been reached or not is still an open question in the open literature. As Osyczka[11] stated, "Is there a universal way of selecting the best performing parameters for all different problems? A genetic algorithm will keep its learning mystery with its parameter dependent solutions."

Optimized Cascade Performance:

The output of the new automated optimization technique is presented and compared with the initial baseline test case in Table 1. The optimized cascade surface Mach-number distribution is compared with initial configuration performance in Fig. 8. A dramatic increase is achieved over the suction side along with a moderate improvement over the last half of the pressure side. The corresponding boundary-layer displacement and momentum thickness for the optimized blade section are also given in Figs. 9 and 10, respectively. Although still relatively small, both displacement and momentum boundary-layer thickness increase in the last quarter portion of the chord. This might be one of the causes of the large increase in the drag coefficient reported in Table 1.

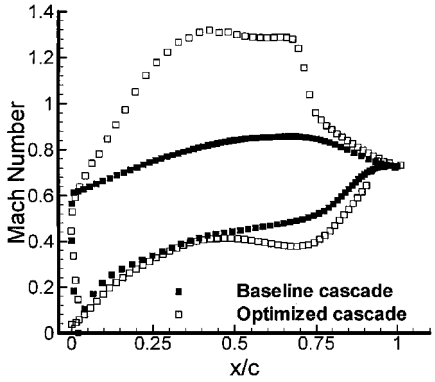

Fig. 8 Cascade surface Mach-number distribution.

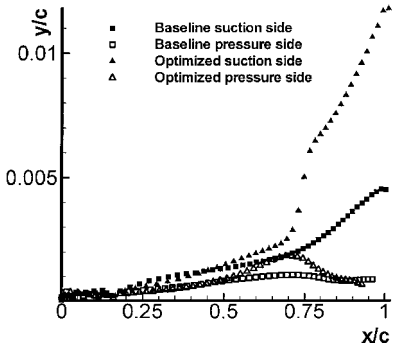

Fig. 9 Boundary-layer displacement thickness distribution.

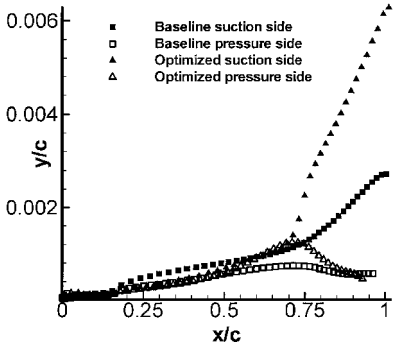

Fig. 10 Boundary-layer momentum thickness distribution.

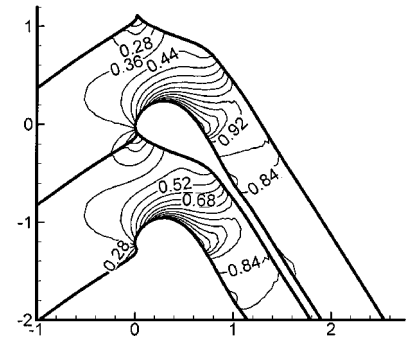

Fig. 11 Mach-number contour for the optimized cascade.

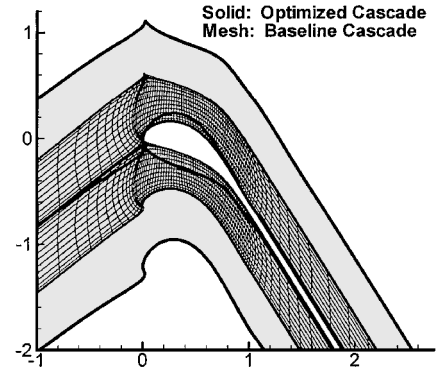

Fig. 12 Cascade geometries of the baseline and optimized blade without C_D constraint.

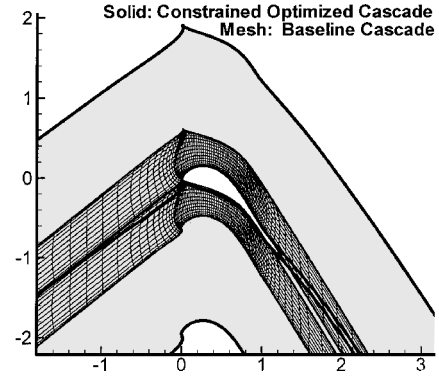

Fig. 13 Cascade geometries of the baseline and optimized blade with C_D constraint.

The corresponding Mach-number contour of the optimized cascade is plotted in Fig. 11. Beginning from a fully subsonic configuration, the flow for the optimized cascade became transonic under increased tangential force. The differences in flow angles, solidity, and thickness between the optimum cascade and the Sanz subcritical cascades are illustrated in Fig. 12.

Because the increased blade loading of the optimized cascade is achieved along with a significant drag increase, an additional drag coefficient constraint is added to the problem. This is attained by adding a penalty term to the objective function as the drag coefficient difference of the baseline and modified cascade. The results of the C_D constrained optimization problem are also shown in Table 1. The results indicate that while incurring a drag very close to the baseline cascade the GA managed to increase the tangential force by more than 13%. The C_D constrained optimized cascade is shown and compared with the baseline cascade in Fig. 13.

Zweifel[12] criterion is an empirical measure of cascade loss, and it emphasizes the effect of solidity on the cascade efficiency. Zweifel has found that the ratio of the actual to an "ideal" tangential blade loading must be approximately 0,8 for minimum loss. He arrived at

this number from a number of experiments on high turning turbine cascades. Actually, this number represents a tradeoff between small spacing of blades with high friction losses and high spacing of blades with poor fluid guidance, ultimately causing high separation. The Zweifel criterion also predicts that the optimum solidity for the test case is around 1.77 (Ref. 13). In the light of this criterion, the optimized cascade solidity is closer to this value than the Sanz supercritical cascade solidity, even though it shoulders a much higher tangential force, indicated in Table 1.

Blade loading results are presented in Table 1. It is seen that the optimization method increases the baseline subsonic cascade tangential force by 124%. Moreover, even when the optimized cascade is compared with the Sanz supercritical cascade, it is seen that the tangential force of the optimized cascade is still higher by 42%. The higher cascade force is achieved by a thicker blade section that might also be good from structural and cooling viewpoints. Also, decrease in solidity will probably lead to a decrease in the number of blades in the turbine, a saving in weight and cost.

Conclusions

A fast and accurate flow solver has been coupled to a fast and robust genetic algorithm so as to optimize the cascade blade loading. The baseline turbine cascade was chosen to be the Sanz subcritical cascade. The main optimization parameters used in the optimization algorithm are the cascade thickness, the solidity, the cascade inlet and exit flow angles. It is shown that as the tangential force increases the flow becomes transonic. Although the surface Mach number of the optimized blade approaches the profile of the Sanz supercritical cascade, this performance increase is achieved with much fewer and thicker blade sections. Despite a higher drag coefficient, the Zweifel criterion predicts that the optimized cascade will also incur less loss when compared to the Sanz supercritical cascade.

References

[1]Ta'asan, S., "Trends In Aerodynamics Design Optimization: A Mathematical Viewpoint," AIAA Paper 95-1731, June 1995.

[2]Blaize, M., Knight, D., and Rasheed, K., "Automated Optimal-Design of 2-Dimensional Supersonic Missile Inlets," *Journal of Propulsion and Power*, Vol. 14, No. 6, 1998, pp. 890–898.

[3]Giles, M. B., and Drela, M., "Two-Dimensional Transonic Aerodynamic Design Method," *AIAA Journal*, Vol. 25, No. 9, 1987, pp. 1199–1206.

[4]Drela, M., "Newton Solution of Coupled Viscous/Inviscid Multielement Airfoil Flows," AIAA Paper 90-1470, June 1990.

[5]Ekici, K., Akmandor, I. S., and Çetinkaya, T., "Quasi-3 Dimensional Analysis and Design of Turbomachinery Blades," AIAA Paper 98-0966, Jan. 1998.

[6]Akmandor, I. S., and Ekici, K., "Airfoil Analysis for Horizontal Axis Wind Turbines," AIAA Paper 98-0020, Jan. 1998.

[7]Denton, J. D., Hirch, Ch., Meauze, G., and Sanz, J. M., "Test Case A/CA-3 Sanz Subcritical Turbine Cascade," *Test Cases for Computation of Internal Flows in Aero Engine Components*, edited by L. Fottner, AGARD-AR-275, Loughton, July 1990, pp. 24, 25.

[8]Obayashi, S., and Takanashi, S., "Genetic Optimization of Target Pressure Distributions for Inverse Design Methods," *AIAA Journal*, Vol. 34, No. 5, 1996, pp. 881–886.

[9]Goldberg, D. E., *Genetic Algorithms in Search, Optimization and Machine Learning*, 1st ed., Addison Wesley Longman, Reading, MA, 1989, p. 237.

[10]Denton, J. D., Hirch, Ch., Meauze, G., and Sanz, J. M., "Test Case A/CA-4 Sanz Supercritical Turbine Cascade," *Test Cases for Computation of Internal Flows in Aero Engine Components*, edited by L. Fottner, AGARD-AR-275, Loughton, July 1990, pp. 26, 27.

[11]Osyczka, A., *Evolutionary Algorithms for Single and Multicriteria Design Optimization*, 1st ed., Springer-Verlag, New York, 2002, pp. 43–46.

[12]Dixon, S. L., *Fluid Mechanics, Thermodynamics of Turbomachinery*, 3rd ed., Pergamon, 1982, pp. 87–89, 128, 129.

[13]Steward, W. L., and Glassman, A. J., "Blade Design," *Turbine Design and Application*, NASA SP-290, Washington, DC, 1973, pp. 113–116.